Vol.26, December.2015 ISSN 2354-7065

Journal of

Ocean, Mechanical and Aerospace

-Science and Engineering-

ISOMAse

International Society of Ocean, Mechanical and Aerospace,
Scientists and Engineers

Journal of Ocean, Mechanical and Aerospace
-Science and Engineering-
Vol.26: December 30, 2015

Contents

ISOMAse

International Society of Ocean, Mechanical and Aerospace
-Scientists and Engineers-

Journal of Ocean, Mechanical and Aerospace
-Science and Engineering-
Vol.26: December 30, 2015

About JOMAse

The **Journal of Ocean, Mechanical and Aerospace -science and engineering- (JOMAse, ISSN: 2354-7065)** is an online professional journal which is published by the International Society of Ocean, Mechanical and Aerospace -scientists and engineers- (ISOMAse), Insya Allah, twelve volumes in a year. The mission of the JOMAse is to foster free and extremely rapid scientific communication across the world wide community. The JOMAse is an original and peer review article that advance the understanding of both science and engineering and its application to the solution of challenges and complex problems in naval architecture, offshore and subsea, machines and control system, aeronautics, satellite and aerospace. The JOMAse is particularly concerned with the demonstration of applied science and innovative engineering solutions to solve specific industrial problems. Original contributions providing insight into the use of computational fluid dynamic, heat transfer, thermodynamics, experimental and analytical, application of finite element, structural and impact mechanics, stress and strain localization and globalization, metal forming, behaviour and application of advanced materials in ocean and aerospace engineering, robotics and control, tribology, materials processing and corrosion generally from the core of the journal contents are encouraged. Articles preferably should focus on the following aspects: new methods or theory or philosophy innovative practices, critical survey or analysis of a subject or topic, new or latest research findings and critical review or evaluation of new discoveries. The authors are required to confirm that their paper has not been submitted to any other journal in English or any other language.

ISOMAse

International Society of Ocean, Mechanical and Aerospace
-Scientists and Engineers-

Journal of Ocean, Mechanical and Aerospace
-Science and Engineering-
Vol.26: December 30, 2015

Scope of JOMAse

The JOMAse welcomes manuscript submissions from academicians, scholars, and practitioners for possible publication from all over the world that meets the general criteria of significance and educational excellence. The scope of the journal is as follows:

- Environment and Safety
- Renewable Energy
- Naval Architecture and Ship Construction
- Computational and Experimental Mechanics
- Hydrodynamic and Aerodynamics
- Noise and Vibration
- Aeronautics and Satellite
- Engineering Materials and Corrosion
- Fluids Mechanics Engineering
- Stress and Structural Modeling
- Manufacturing and Industrial Engineering
- Robotics and Control
- Heat Transfer and Thermal
- Power Plant Engineering
- Risk and Reliability
- Case studies and Critical reviews

The International Society of Ocean, Mechanical and Aerospace –science and engineering is inviting you to submit your manuscript(s) to admin@isomase.org for publication. Our objective is to inform authors of the decision on their manuscript(s) within 2 weeks of submission. Following acceptance, a paper will normally be published in the next online issue.

ISOMAse

International Society of Ocean, Mechanical and Aerospace
-Scientists and Engineers-

Journal of Ocean, Mechanical and Aerospace
-Science and Engineering-
Vol.26: December 30, 2015

Editors

ISOMAse

International Society of Ocean, Mechanical and Aerospace
-Scientists and Engineers-

Journal of Subsea and Offshore
-Science and Engineering-, Vol.26

December 30, 2015

Undercarriage Design of Excavator Model in Application of Various Track Drive

Nazaruddin,[a] and Kiki[a], Gunawan[a]

[a)] Laboratorium Hidrolik dan Pneumatik, Jurusan Teknik Mesin, Fakultas Teknik Universitas Riau
*Corresponding author: nazaruddin.unri@yahoo.com

Paper History

Received: 11-November-2015
Received in revised form: 30-November-2015
Accepted: 30-December-2015

ABSTRACT

The excavator is the units of the heavy equipment that serves the physical development sectors such as mining excavations in the area, establishing or expanding roads and expand agricultural land and other physical development . One part of the excavator that has a very large role in the undercarriage . Undercarriage is a component of the heavy equipment that serves as a driver and has a track drive right and left track drive . This research was conducted with the aim to make modeling as excavators in general by using materials available in the market. Next, calculate the speed , direction of turn with a different variation of the track (ceramic , asphalt , soil) and the maximum tilt angle that can be achieved by the excavator . From the test data and calculations have been carried out with 3 times the gear reduction is obtained without load speed excavator bucket is 0.25 m/s while using a load of 1.5 kg bucket excavator speed is 0.24 m/s at the track ceramics . While the direction of maximum inflection occurs on the track with a diameter ceramic to turn right for 995 mm and 782 mm turn left. At the maximum angle of incline can be obtained at 10 degrees .

KEY WORDS: *Undercarriage; Track Drive; Excavator*

1.0 INTRODUCTION

Excavator is one of heavy equipment to carry out the various of construction such highway, canal, agriculture and mining project. The using of the excavator is to accelerate the construction process and save the consuming time in construction and operation process in order to reduce cost. In this study, the effort to obtain the optimum heavy equipment is continuously done in order to maximize the operation of excavator by modification of undercarriage part[1]. As shown in figure 1.1

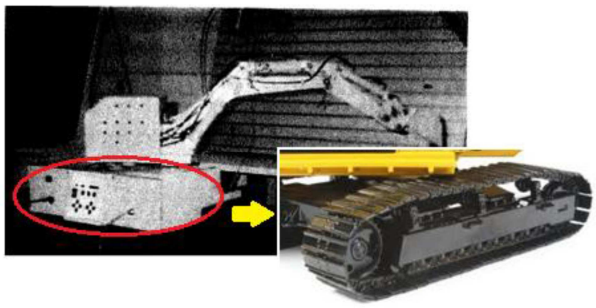

Figure 1.1 Excavator models that will be modified[1]

2.0 THEORY

Undercarriage is essential part of excavator which consists of several component to support the movement of excavator such as sprocket, final drive unit, track shoe, track link, track frame, track roller, front idler as shown in figure 2.2,

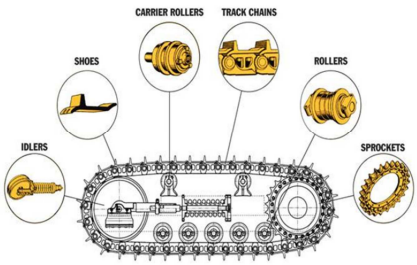

Figure 2.2 Undercarriage Component [4]

Final drive unit is set in the undercarriage that consists of gear and planetary gear units where transmit the power from the engine and increasing the torque. In this study, the final drive is discribed as follow:

2.1. Spur Gear

Spur gears, illustrated in Fig. 2.3, have teeth parallel to the axis of rotation and are used to transmit motion from one shaft to another, parallel, shaft. Of all types, the spur gear is the simplest and, for this reason, will be used to develop the primary kinematic relationships of the tooth form[5]. In addition, the spur gears are applied in many devices like electric screwdriver, oscillating sprinkler, windup alarm clock, washing machine and clothes dryer.

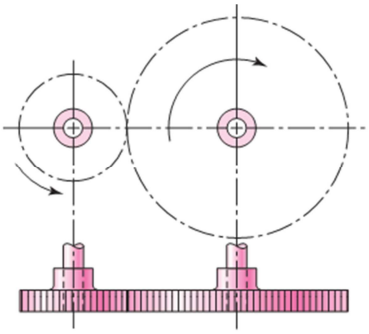

Figure 2.3 Spur Gear

2.2 Bevel Gear

Bevel gears, shown in Fig. 2.4, have teeth formed on conical surfaces and are used mostly for transmitting motion between intersecting shafts. The figure actually illustrates *straight-tooth bevel gears*. *Spiral bevel gears* are cut so the tooth is no longer straight, but forms a circular arc[5]. *Hypoid gears* are quite similar to spiral bevel gears except that the shafts are offset and nonintersecting.

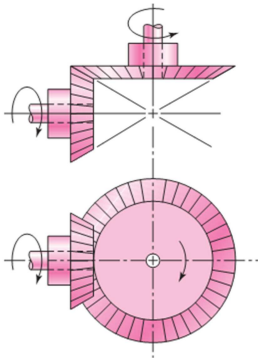

Figure 2.4 Bevel Gear

2.3 Sprocket and Chain

Sprocket is one of machine element which profiles wheel with teeth and using a chain in order to transmit the power. It is distinguished from a gear which directly contact to a counter gear, and differ from pulley which has smooth surface and using a belt to transmit the power. A chain is series of link which assemble with sprocket in transmission of power without slip.

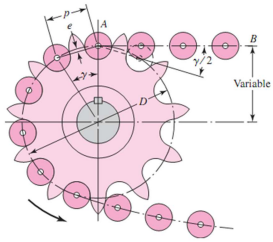

Figure 2.5 Illustration of Sprocket and Chain [5]

2.4 Electric Motor

Electric motor is a part of component to drive fan, compressor, pump which source from electrical power. The electric motor is classified into two types of motor such as DC Motor and AC Motor. The circuit of DC motor can be configured as below:

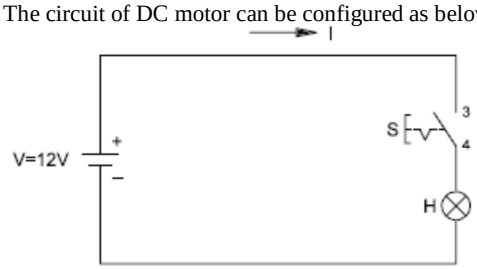

Figure 2.5 Electrical Circuit of DC Motor

3.0 RESEARCH METHODOLOGY

This research conducted three steps of process

3.1 Undercarriage Design

Undercarriage design carried out following the flowchart below:

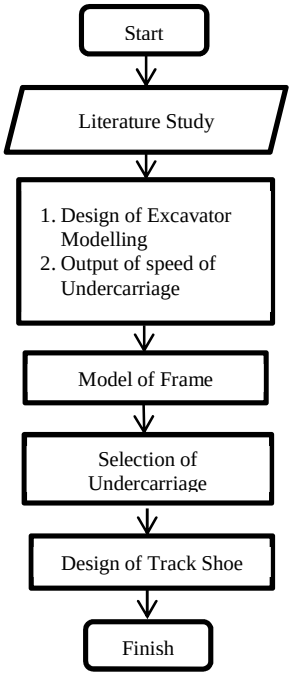

Figure 3.1 Flowchart of Undercarriage Design

The dimensions of the undercarriage were taken from 1:14 scaled model of the actual size so structured such that generates the layout as in Figure 3.2 below

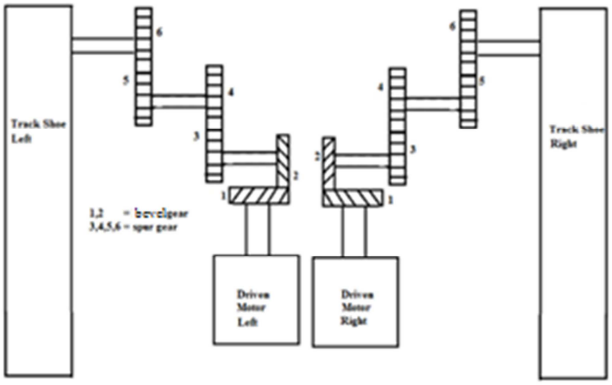

Figure 3.2 Layout of Power Transmission of Undercarriage

Power transmission from driven motor to each track shoe using a pair of bevel gear (gear 1 and gear 2) and two pairs of spur gears (pinion gears 3 to 6).

The layout made its CAD drawings into 3D models as shown in Figure 3.3 below

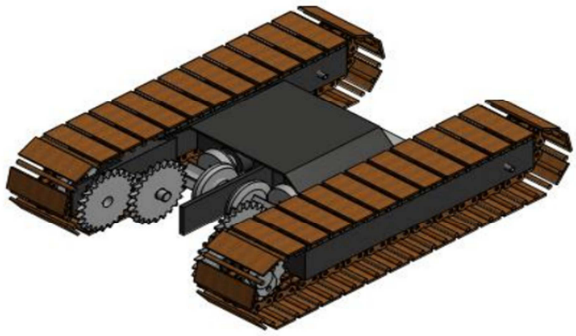

Figure 3.3 Result of 3D Design of Undercarriage

The transmission arrangement to obtain the undercarriage low speed of 3.6 km/h and undercarriage hight speed 5.5 km/ as the speed of the excavator is generally where a motor driven rotation of 2000 rpm

3.2 Undercarriage Fabrication

The process of making undercarriage conducted at the Laboratory of Production of Mechanical Engineering, University of Riau. Flow chart of the manufacturing process can be seen in Figure 3.5.

Making the frame by means of Steel box cut using grinding pieces with a length of 30 cm. Then one end of the steel box section is cut 10 cm with the aim to include idler and tension to set the track shoe and make the position of bearing needed to simplify and expedite the undercarriage in the running

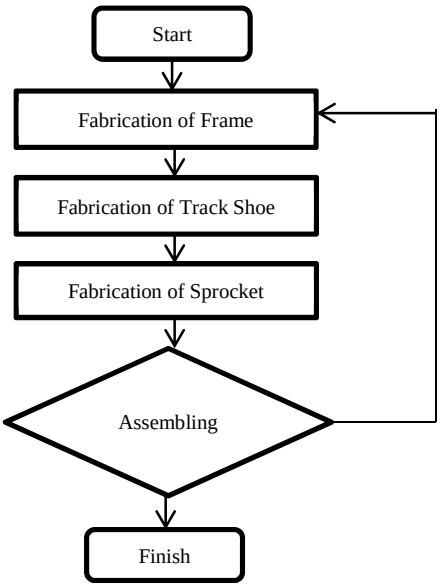

Figure 3.4 Flowchart of Fabrication

Track shoe is made by cutting a plate that has a thickness of 2 mm and a length of 50 mm and a width of 15 mm. Plates that have been cut was installed in the cracks of the iron cylinder has been connected with the chain sprocket. Furthermore, the merger between the chain sprocket or the so-called track shoe with a steel box that has been cut. The result as in Fig. 3.5

Figure 3.5 Assembling of Track Shoe

Installation of the sprockets and gears. After completion of the formation of the frame, the next step is the process of turning to make the position of the gear and then making a connection between the position of the gear to the frame (see in Fig. 3.6). The gears used are gears that are easy to obtain, is composed of two types of gears is a hypoid gear and spur gear and performed 3 times to get a final speed reducer such as undercarriage in general.

(a) The position of the gear (b) Sprocket and gear on the frame

Figure 3.6 Installation Stand Gear and Sprocket on Frame

3.3 Undercarriage Testing

At this stage we will perform an undercarriage testing activities. This process can be seen in Fig. 3.7 following a flow chart of the testing process.

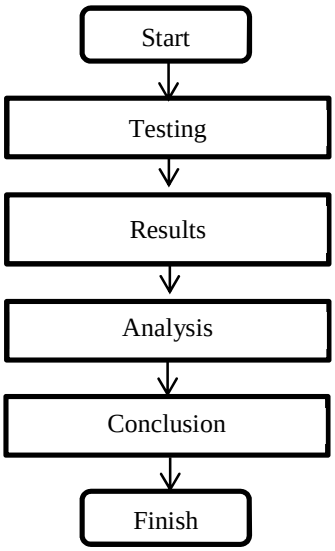

Figure 3.7 Flowchart of Undercarriage Testing

This test was conducted to determine the outcome of designing and manufacturing has been done. Testing is done with three types of tests, among others:

1. Testing speed and a final round of undercarriage
   This test was conducted to determine the speed and the final round of the excavator. Testing is done by giving the mileage on the excavator which was then measured how long it takes the excavator. And rotation speed testing is done with 3 variations of the track are: ceramics, asphalt and soil. While the rotation speed is obtained from then converted into angular velocity rounds finally obtained value.

2. Testing the direction of turn undercarriage
   This test is done to determine how much deflection angle that can be done by the excavator. Testing is also done with a variation of 3 tracks namely: ceramics, asphalt and soil (see in Fig. 3.8)

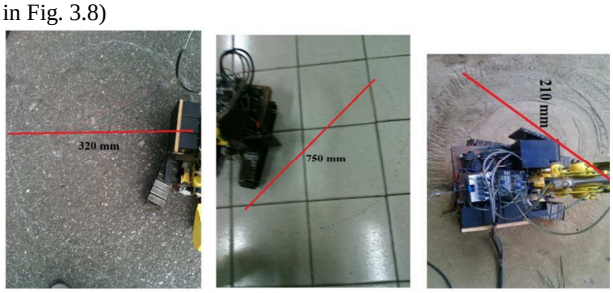

Figure 3.8 Testing Direction Turn

3. Tests on inclined plane.
   This test is done to determine how much the maximum angle that can be taken by the excavator. Testing was done with 6 variation of the angle that is 5°, 10°, 15°, 20° and 25° (see in Fig. 3.9)

Figure 3.9 Comparison Testing on inclined plane

4.0 RESULT AND DISCUSSION

The testing had been conducted to obtained the data of speed and excavator's manouver in several models of track like ceramic, asphalt and land.

In Aspalth Track

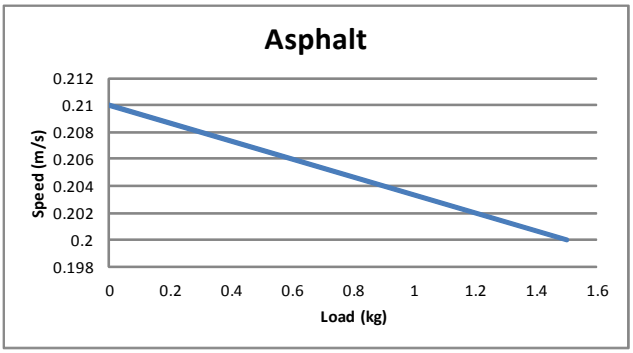

Figure 4.1 Load vs Speed in Asphalt Track

In the Figure 4.1 show the result of undercarriage experiment in the asphalt track, where the increasing of loads cause the speed of excavator decreased. Figure 4.2 illustrate the load vs rotation as well, the increasing of load affect to the rotation of undercarriage final drive.

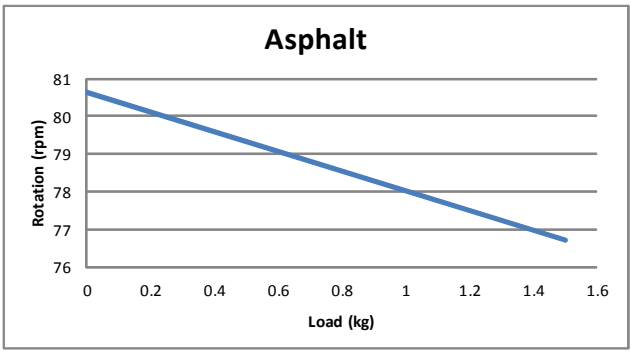

Figure 4.2 Load vs Rotation in Asphalt Track

In Ceramic Track

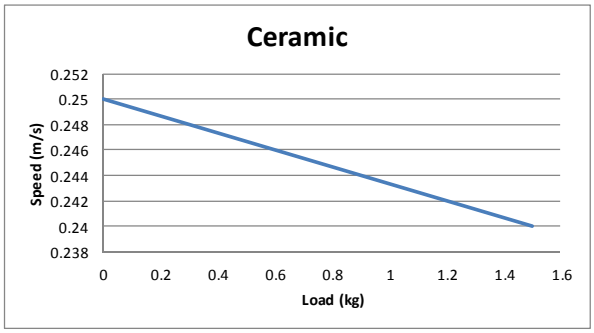

Figure 4.3 Load vs Speed in Ceramic Track

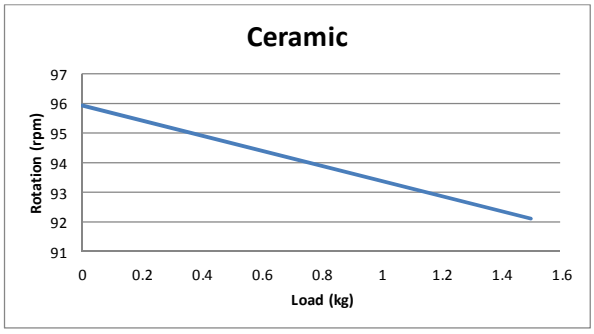

Figure 4.4 Load vs Rotation In Ceramic Track

In the ceramic track as shown in figure 4.3 shows the speed of excavator against the increasing of load, where the speed linearly decrease. The figure 4.4 shows the rotation of undercarriage decrease by increasing of load.

In Unpaved Road

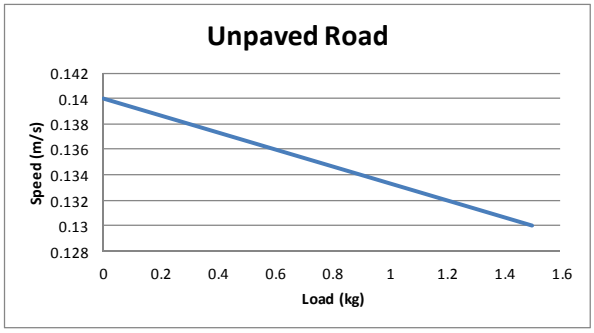

Figure 4.5 Load vs Speed in Unpaved Road

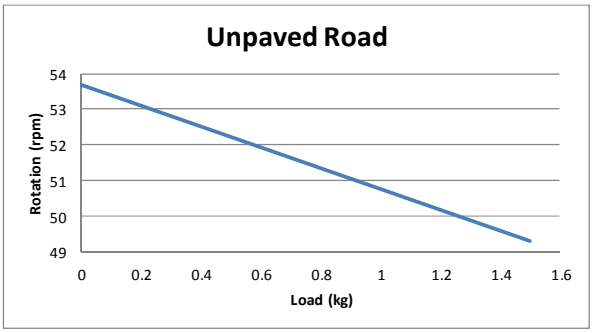

Figure 4.6 Load vs Rotation in Unpaved Road

In the figure 4.5 show the comparison between load and speed in unpaved road. It indicates the speed of excavator on unpaved road track is the lowest speed when compare to other track, as well as the rotation of undercarriage final drive become decreasing by increasing of load.

5.0 CONCLUSION

From the results of the design, manufacture and calculations have been performed, then obtained some conclusions of a thesis entitled designing and manufacturing excavator undercarriage components on the model in the Laboratory of Hydraulic and Pneumatic University of Riau, namely:

1. Provided the form of the undercarriage of the design and manufacturing has been done with the long dimension of undercarriage 331 mm, width 234 mm and height 78.6 mm
2. From the test results that have been done so by doing three times the reduction of the gear system and using the motor power windows Toyota gained speed as the excavator excavator generally is 3.6 km / h or 1 m / s for low speed undercarriage and 5 , 5 km / h or 1.5 m / s for high speed undercarriage.
3. From the examination of the direction of turn can do the undercarriage on the track asphalt, ceramics and soil the minimum diameter are on the track of land with a diameter of 210 mm.
4. The maximum slope that can be achieved excavator which is 10 degrees with a power of 83.60 Watts.
5. Obtained a modified cable remote control to move the undercarriage..

REFERENCE

1. Julianto and Nazaruddin, 2004, Perencanaan dan Pengujian Model *Excavator*, Kertas Karya Prodi D3 Teknik Mesin Universitas Riau.
2. Jati, Hidayah, 2011. Peningkatan Perawatan Komponen *Undercarriage* Alat Berat. Depok: Universitas Indonesia.
3. Prasetyo, Deta. 2010. Pembuatan Alat Praktikum Perawatan Sistem Transmisi Roda Gigi. Surakarta : Universitas Sebelas Maret
4. Soleh, Muhammad. 2005. Sistem Operasi dan Perawatan *Travel* Motor pada *Excavator* Hitachi Zaxis-200, Prodi D3 Teknik Mesin Universitas Riau.

5. Shigley, 2006, Mechanical Engineering Design 8th, McGraw-Hill Companies, USA

Journal of Ocean, Mechanical and Aerospace
-Science and Engineering-, Vol.26

December 30, 2015

Rock Mass, Geotechnical and Rock Type Identification Using SASW and MASW Methods at Kajang Rock Quarry, Semenyih, Selangor Darul Ehsan

Husnul Kausarian,[a*]

[a)] *Engineering Geology, Universitas Islam Riau, Indonesia*

*Corresponding author: kausarianhusnul@yahoo.com

Paper History

Received: 16-November-2015
Received in revised form: 28-December-2015
Accepted: 30-December-2015

ABSTRACT

Rock mass characterization study at Kajang Rock quarry was performed using Spectral Analysis of Surface Waves (SASW) and Multichannel Analysis of Surface Waves (MASW) methods. Rock Quality Designation (RQD) can be measured in the field directly. Discontinuity and processing survey methods determined from 4 locations that have been examined in this study area. Based on MASW and SASW methods, velocity of S waves (Vs) can be obtained and weathering grade of rock mass has been classified. Location 1 consists of 5 weathering zones, SASW data indicates surface wave velocity (Vs) obtained from 198 m/s to 2044 m/s, MASW (Vs) ranges obtained from <600 m/s to> 2400 m/s. Location 2 consists of 4 weathering zones, (Vs) of SASW obtained from 592 m/s to 2271 m/s and (Vs) of MASW obtained from 400 to 2000 m/s. Location 3 consists of 4 weathering zones with (Vs) of SASW obtained from 512 m/s to 2465 m/s and (Vs) of MASW obtained from 400 to >1200 m/s. Location 4 consists of 5 weathering grades with (Vs) of SASW obtained from the 200 m/s to 2040 m/s and (Vs) of MASW obtained from 300 to >2300 m/s. Rock Quality Designation (RQD) in Location 1 shown the rock quality is excellent (98.63%), in Location 2, RQD shows the rock is good (98.38%), in Location 3 RQD shows the rock is excellent (99.03%), in Location 4 RQD shows the rock is excellent (96.43%).

KEY WORDS: *Kajang Rock Quarry; SASW; MASW; RQD.*

NOMENCLATURE

SASW	Spectral Analysis of Surface Waves
MASW	Multichannel Analysis of Surface Waves
RQD	Rock Quality Designation
Vp	Velocity of P Wave
Vs	Velocity of S Wave
m/s	Meter per second
SG1,2 ...	Location survey 1,2 …
Vr	Rayleigh velocity
λ	Wavelength
Z	Depth
μ	Poison ratio
C	Constant value depends on Poison ratio
G	Shear modulus
ρ	Density

1.0 INTRODUCTION

This study area located at Kajang Rock quarry, Semenyih (Figure 1) and the quarry is a granite rock quarry (Figure 2). Kajang Rock Quarry located in the Semenyih district, Selangor. The quarry located at Longitude 02º55,261' and Latitude 101°50,376' at the north of Semenyih district. Semenyih has many parishes quarry, it is visible from many former quarries in the outskirts town area and also at the hills area of this district.

Lithology at the quarry is granitic type. The study focused on the fresh rock and weathered granite only. Position of the study area is located in the middle line of the granite pluton body, and only one type of lithology detected in this area.

Surveyed locations are slopes of a quarry outcrop which known as Terrace 2 (SG1 (Location 1) and SG2 (location 2)), Terrace 5 (SG 3 (Location 3)) and terrace 8 (SG4 (Location 4)) (Figure 3). Studies were conducted on the quarry outcrop at the inactivity, which is not operational in the short term.

Geographical condition near the quarry is oil palm plantation. However, a highway was built near the quarry, the road linked the Reko highway, Kajang, Semenyih, Kuala Lumpur and Sungai Long. These highways known as Kajang Silk Highway.

1.1 Literature Review

Ahya (2007) states that the granite at Km 14.6 of SILK highway composed by grade I and I-II and has coarse to medium texture. Ahya also find Rock Quality Designation (RQD) is 87.73%. Ser (2007) states the granite in Kajang Rock quarry consists of five types of granite, which are medium-coarse-grained porphyry granite, moderately coarse-grained granite, biotite granite, fine grain sheared white granite, clorite sheared granite. Ser centralize analysis of rock mass characterization and rock quality that found this area is starting from very low (V) to very good (I), but most are concentrated in low quality (IV) to moderate (III). Ser also states that the rock mass classification system based on RMR Bieniawski 1979, found 44% of the rock mass is in good quality (class II) and 56% of average quality (Class III). Husnul (2013) states the condition of granitic rock in this area is in good condition to be quarried.

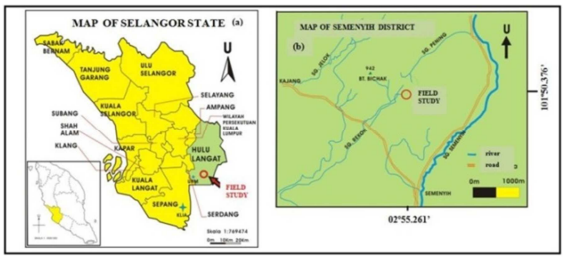

Figure 1: (a) Map of Selangor State, (b) Semenyih District Map.

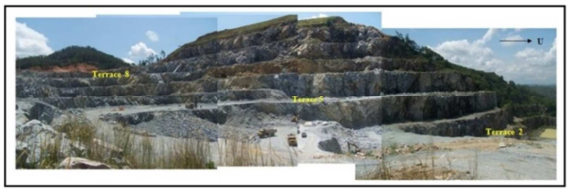

Figure 2: Field study area (terrace) at Kajang Rock Quarry.

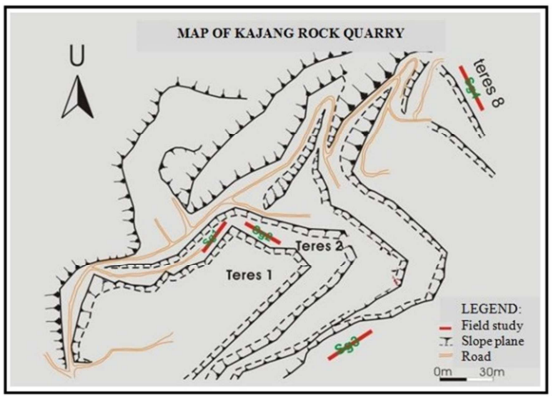

Figure 3: Plan view of field study location (Sg1, Sg2, Sg 3, Sg4), Kajang Rock Quarry, Semenyih (Modified from Ser, 2007).

2.0 OBJECTIVES

The main purpose of this study is to determine the effectiveness of SASW and MASW methods to characterize of igneous rock mass in this study area. The main objectives of this study are:

1. Characterize the granitic rocks in Kajang Rock quarry using SASW and MASW geophysical methods.
2. Determine the Rock Quality Designation (RQD) for granitic rocks using geophysical methods used in the study area.
3. Determine RQD on the discontinuity of the granite rock and rock quality indicator to compare RQD from the geophysical methods used.

3.0 METHODOLOGY

3.1 Principal of Seismic Method

SASW has been introduced since the 1980s. SASW has the advantages like this method is fast, inexpensive and nondestructive characterization studies in geotechnical and construction sites. Heisey (1982), Nazarian and Stokoe (1984), Tokimatsu et al (1991) and Mathews et al (1996) have been developed this method.

The development of the latest technique is multi-channel analysis of surface waves (MASW) where it mixes SASW and seismic reflection techniques. This technique developed in Kansas Geological Survey (Park et al 1999), can produce two-dimensional data where SASW can only produce one dimension only.

In addition to the body wave moving in an elastic medium, there is another wave that propagates in elastic media surface called surface wave. In the method of spectral analysis of surface waves (SASW), Rayleigh wave velocity is determined and reversed a shear wave velocity, Vs. Relationship between Vs and Vr as shown by equation (1-5) in elastic media.

$$Vr = f\lambda \quad (1)$$

$$Z = \lambda/2 \quad (2)$$

$$Vr = CVs \quad (3)$$

$$G = \rho Vs^2 \quad (4)$$

$$C^6 - 8C^4 + \left[3 - \frac{1-2\mu}{1-\mu}\right]C^2 + 16\left[\frac{1-2\mu}{2(1-\mu)}\right] = 0 \quad (5)$$

Where f is frequency, λ is wavelength from source to detector, Z is depth, C is constant value depends on Poison ratio, G is Shear modulus, ρ is density and μ is Poison ratio.

Deere (1964) suggests the Rock Quality Designation (RQD) as a density discontinuity parameter obtained from drill core. Deere define RQD as cumulative core length of more than 10 cm for a long drilling unit, as shown in equation (6)

$$RQD = \frac{Cumulative\ length\ of\ rock\ cores > 10cm}{Total\ length\ of\ rock\ cores} X100\% \quad (6)$$

3.2 Software and Operation Equipment

Hammer hit to the steel plate that is attached to the surface of the soil used to generate waves that will propagates in subsurface, the main wave generated is Rayleigh wave. The frequency range of Rayleigh wave has sufficient energy to be detected by the sensor

by using some type of hammer that has a different weight. Rayleigh wave detection will be carried out from geophones or acceleration transducer (accelerometer) which is connected to a spectrum analyzer.

The spectrum analyzer will record data such as wave spectra and phase coherent functions in file format *.txt. The data will be displayed by using Mircosoft Excel and saved in *.txt file format. WinSASW 2.0 software was used to generate the curve of dispersion (Dispersion Curve) using that *.txt file and produce a graft of Rayleigh wave velocity (Vr) against wavelength (λ). Next, the dispersion curve inverted to be shear wave velocity (Vs) versus depth graft using WinSASW 2.0. Shear modulus or Young's modulus is calculated based on shear wave velocity (Vs) obtained from the inverse scattering income stiffness profile. The following discussion will be focused on equipment SASW in the field and several factors need to be considered to start the test SASW the choice of wave source, type of detector and the distance among the detector.

The equipment that was used for seismic studies in the area is Terraloc ABEM Mark 6, 24 geophones, two connection cables 12 buttons, hammer with many weight types, HITACHI Battery HG44-12 and battery charger, steel plates and compass to measure the direction of survey line.

Total of four line surveys were carried out with range 69 meters each. Total of 24 geophones arranged in a straight line profile with distance 3m between. Battery used to supply current and operates the equipment; ABEM Terraloc Mark 6. Each line profile has carried out seven times of emission wavelength on the relative distances specified (Table 1). The source waves generated from the hammer on a piece of steel plate with a vertical shock.

Table 1: Configuration of shock causes from the first geophone.

No. of Shock	Distance (Meter)
1	-10
2	1.5
3	6.5
4	34.5

3.3 Rock Quality Designation (RQD)

Calculation of RQD values in the field can be obtained by the discontinuity survey technique, this technique is more systematically. Based on this technique, the scanning line is made on outcrop horizontally and vertically. Vertical scan line is made in the intervening at several meters and perpendicular to the horizontal scan lines. Interval width depends on the density of the discontinuity sets to obtain the required data as shown in Figure 4.

Figure 4: Line of discontinuity in vertical scanning survey.

4.0 RESULT AND DISCUSSION

4.1 Profile of Location 1

Based on relationship between rock material with shear wave velocity (Bay 2000) (Table 2), (Vs) of Spectral Analysis of Surface Waves (SASW) profile at Location 1 (Figure 5) shows at the depth between 0-0.13 m. Vs indicates a lower value between 198 m/s - 1300 m/s, represents the existence of hard soil, mix of hard soil and granite which have experienced weathered process. At the depth 0.13 to 1.34 m shows layer of highly weathered granite with Vs ranging from 1025 to 1300 m/s, while at the depth of 1.34 to 7.15 m indicates the existence of fresh granite layer that has high Vs between 2014 m/s - 2044 m/s.

Vs of Multichannel Analysis of Surface Waves (MASW) profile at Location 1 (Figure 6) has a range of Vs from <600 - >2400 m/s with depth reached into 12 meters. Location 1 consists of 3 main zones. The first zone has Vs 400-1000 m/s with the depth of 3 m. Vs at second zone has 1000 - 2000 m/s and the thickness estimation is 7 m. Third zone has a range of Vs from 2000 to 2400 m/s, this zone was detected at the depth of 10 m below.

Table 2: relationship between rock materials with shear wave velocity

Rock Material Classification	Velocity of shear wave, Vs (m/s)
Very soft	84-107
Soft Soil	107-137
Moderately Soft Soil	137-183
Hard Soil	183-274
Very Hard Soil	274-366
Highly Wheatered Rock	366-610
Slightly Wheatered Rock	610-2743

4.2 Profile of Location 2

SASW profile at Location 2 (Figure 7) shows the depth between 0-0.06 m, Vs indicates between 592 m/s - 593 m/s, represents the existence of high weathered granite rocks. At the depth of 0.06 - 13.60 m indicates the existence of fresh granite layer that has high Vs between 1407 m/s - 2271 m/s.

MASW profile at Location 2 (Figure 8), has a range of Vs from 400 to 2000 m/s and the depth reached 10 m. Location 2 consists of 3 main zones, the top zone has Vs ranges from 400 - 750 m/s with 3.5 m deep. The second Zone has Vs ranges 750 - 1250 m/s and 4.5 meters deep. The third zone has Vs ranges 1250 to 2000 m/s, this zone was detected at the depth of 8 m below.

4.3 Profile of Location 3

At the depth of 0 - 0.76 m Vs indicates from 512 to 1132 m/s, represents the existence of high, medium and low weathered granite. At the depth of 0.76 - 3.94 m indicates the existence of medium weathered granite layer with Vs ranges from 1499 to 1504 m/s, fresh rock found at 3.94 - 10.94 m depth and has a high Vs between 1504 m/s - 2465 m/s. Figure 9 shows the profile of Vs at Location 3.

Figure 10 shows the profile of MASW at Location 3, has Vs ranges from 400 - >1200 m/s and reached 10 m of depth. Location 3 consists of 3 main zones. The top zone has Vs ranges 400-600 m/s with approximate depth of 4 m. Second zone has Vs ranges 600 - 1000 m/s and 4 m depth. The third zone has Vs ranges from 1000 to 1200 m/s, this zone detected at the depth of 8 m.

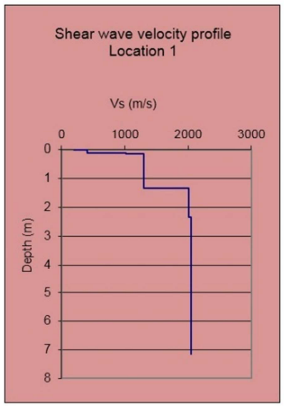

Depth (m)	Vs (m/s)
0.00	198
0.01	198
0.01	406
0.11	406
0.11	1025
0.12	1025
0.12	1025
0.13	1025
0.13	1300
1.34	1300
1.34	2014
2.35	2014
2.35	2044
3.75	2044
3.75	2044
5.35	2044
5.35	2044
7.15	2044
7.15	2044

Figure 5: Shear wave velocity (Vs) profile at Location 1.

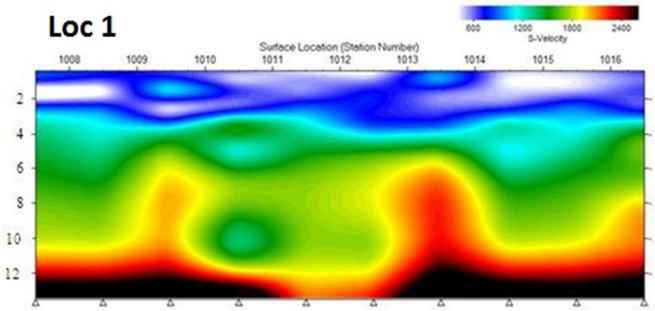

Figure 6: (Vs) MASW Profile at Location 1.

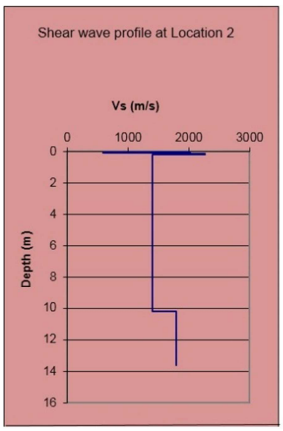

Depth (m)	Vs (m/s)
0.00	592
0.03	592
0.03	593
0.06	593
0.06	1463
0.09	1463
0.09	1918
0.11	1918
0.11	2261
0.15	2261
0.15	2271
0.20	2271
0.20	1407
10.20	1407
10.20	1798
11.80	1798
11.80	1798
13.60	1798
13.60	1798

Figure 7: Shear wave velocity (Vs) profile at Location 2.

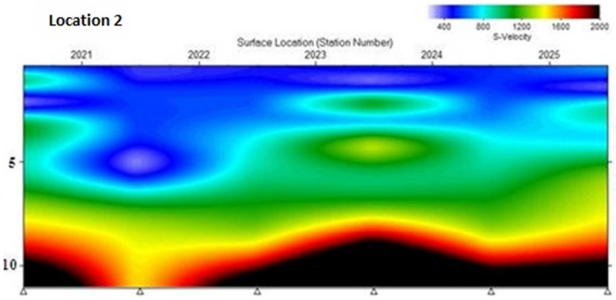

Figure 8: (Vs) MASW Profile at Location 2.

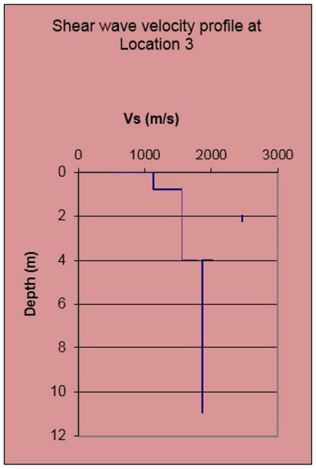

Depth (m)	Vs (m/s)
0.00	512
0.01	512
0.01	1132
0.76	1132
0.76	1499
2.61	1499
2.61	1504
3.94	1504
3.94	1871
4.94	1871
4.94	1871
6.14	1871
6.14	1871
7.54	1871
7.54	1871
9.14	1871
9.14	1871
10.94	1871

Figure 9: Shear wave velocity (Vs) profile at Location 3.

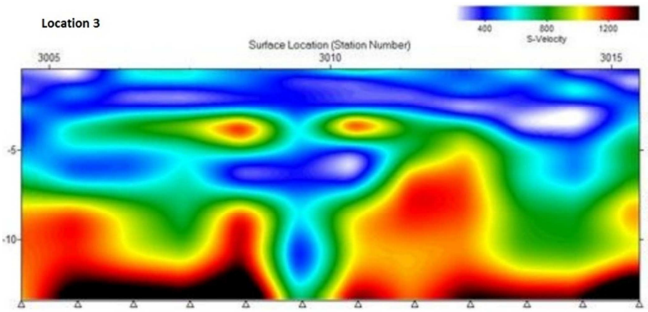

Figure 10: (Vs) MASW Profile at Location 3.

4.4 Profile of Location 4

Figure 11 shows the profile of Vs at this location. At the depth between 0 - 0.13 m Vs indicates between 200 m/s - 1320 m/s, represents the existence of hard soil, very hard soil and granitic rocks with slight/medium weathered. At the depth of 0.13 to 7.15 m, indicates the existence of fresh granite layer that has Vs between 2010 m/s - 2040 m/s.

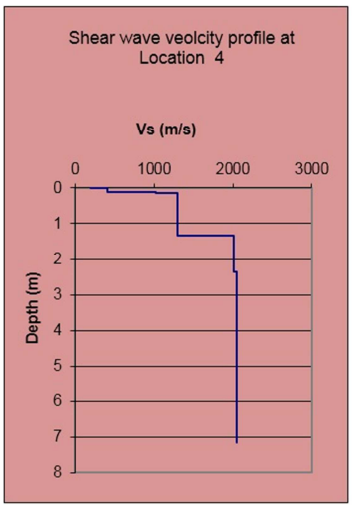

Depth (m)	Vs (m/s)
0.00	200
0.01	200
0.01	408
0.11	408
0.11	1030
0.12	1030
0.12	1030
0.13	1030
0.13	1320
1.34	1320
1.34	2010
2.35	2014
2.35	2040
3.75	2040
3.75	2040
5.35	2040
5.35	2040
7.15	2040
7.15	2040

Figure 11: Shear wave velocity (Vs) profile at Location 4.

Figure 12 shows the profile MASW in Location 4, has a range of Vs ranges from 300 to 2300 m/s and reached 8 m depth. Location 4 consists of 3 main zones. The top zone has Vs 300 - 800 m/s with an approximate depth of 1 m. Second zone has Vs 800 - 1400 m/s with depth estimation is 4 m. The third zone has Vs ranges from 1400 to 2300 m/s, this zone is detected at the depth of 5-8 m below.

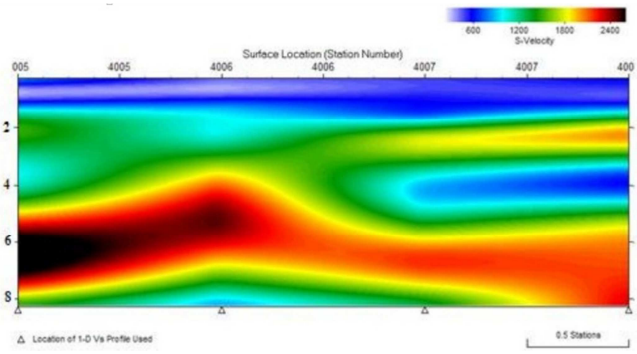

Figure 12: (Vs) MASW Profile at Location 4.

4.5 Profile of Rock Quality Designation (RQD)

To obtain more effective RQDdiscontinuity (Figure 13), a total of four discontinuity survey was conducted in the study area. RQDdiscontinuity value obtained from 98.63%, 98.38%, 99.03% and 96.43% and has very good rock mass quality standard in accordance with Deere (1968). From study location, the existence of discontinuity represented by very hard soil and weathered rock on the depth of 0.0-0.1 m. At the depth of 0.1-7.4 m, it was composed of fresh and a few weathered granite rocks.

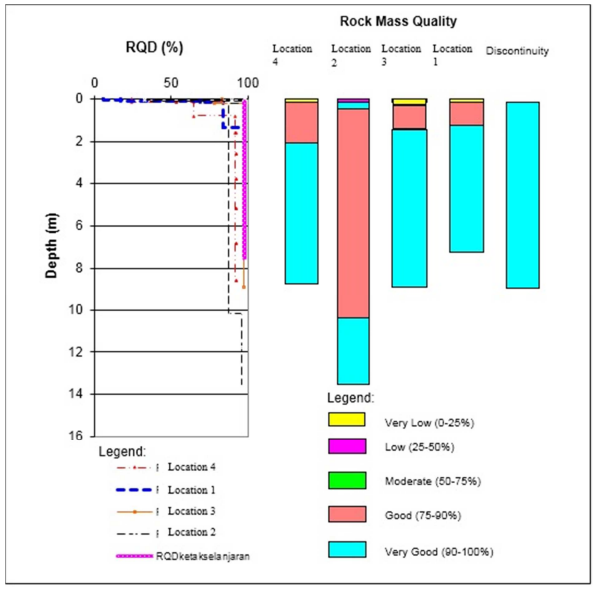

Figure 13: Rock Quality Designation (RQD) measurement at Kajang Rock Quarry.

5.0 CONCLUSION

SASW data shown the subsurface layers of this study area clearly, which consists of hard soil, very hard soil, granite rocks with slight/medium weathered (0 - 0.13 m depth), and fresh granite rock (0.13 to 7.15 m depth). The result from MASW has Vs ranges from 400-1000 m/s, found at 3 m depth and at the depth of 3 - 10 m has Vs ranges from 1000 - 2000 m/s. At the depth of 10 m below, Vs ranges from 2000 to 2400 m/s. As the average, the value of fresh granitic rocks RQD survey line is 98.63%.

Overall, Spectral Analysis of Surface Waves (SASW) and Multichannel Analysis of Surface Waves (MASW) methods helped to map the subsurface condition, especially for the granite rock area. Comparison with Rock Quality Designation (RQD) data, the differentiation is not too much, means these methods become trustable to use.

ACKNOWLEDGEMENT

The authors would like to convey a great appreciation to collaboration networking between Universitas Islam Riau and Universiti Kebangsaan Malaysia for supporting this research.

REFERENCE

1. Bay, J. A. 2000. Site characterization using the spectral analysis of surface waves method. Seminar at University of Alabama at Birmingham.
2. Deere, D.U. 1968. *Geological Considerations, Rock Mechanics in Engineering Practice*. New York: Wiley.
3. Faizatul Ahya. 2007. *Kestabilan cerun di KM 14.6 Lebuhraya SILK, Hulu Langat, Selangor.* Undergraduate Thesis. National University of Malaysia.
4. Heisey, J.S. 1982. Determination of in situ shear wave velocity from spectral analysis of surface waves. Tesis M. Sc. University of Texas.
5. Husnul Kausarian, abdul rahim shamsudin, yuniarti yuskar. 2014. Geotechnical and Rock Mass Characterization Using Seismic Refraction Method At Kajang Rock Quarry, Semenyih, Selangor Darul Ehsan. Journal of Ocean, Mechanical and Aerospace-Science and Engineering-, Vol. 13.
6. ISRM. 1981. *Rock characterization, testing and monitoring.* In ISRM suggested Methods, Brown, E.T (ed.) Oxford: Pergamon Press.
7. Matthews, M.C., Hope, V.S. & Clayton, C.R.I. 1996. The geotechnical value of ground stiffness determined using seismic methods. *Proc. Of 30th Annual Conference of the Engineering Group of the Geological Society*: 1-11.
8. Mohd Azmi Ismail, Khairul Anuar Mohd Nayan, Abdul Rahim Samsudin & Abdul Ghani Rafek 2001. *Spectral analysis of surface waves method: an initial assessment and its potential use in geology.* Geological Society of Malaysia Annual Geological Conference: 185-190.
9. Mohd Khairul Azmi. 2007. *Anistoropi seismos batuan granit sebagai penunjuk kualitatif orientasi ketakselanjaran utama.* Master Tesis, Universiti Kebangsaan Malaysia.
10. Nazarian, S. & Stokoe, K.H.II. 1984. In situ shear wave velocity from spectral analysis of surface waves. *Proc. of 8th World Conference on Earthquarke Engineering* 3:31-38.
11. Park, C. B., Miller, R.D. & Xia, J. 1999. Multichannel analysis of surface waves. *Geophysics* 64(3):800-808.
12. Priest, S.D. 1993. *Discontinuity Analysis for Rock Engineering.* London: Chapman & Hall.
13. Ser Kong Aik. 2007. *Pencirian geomekanik jasad batuan granit, kuari Kajang Rock di mukim Semenyih, Hulu Langat, Selangor Darul Ehsan.* Undergraduate Thesis. National University of Malaysia.
14. Sjogren, B., Ofsthus, A. & Sandberg, J. 1979. *Seismic classification of rock mass qualities.* Geophysical Prospecting 27(2): 409-442.
15. Suharsono, Abdul Rahim Samsudin & Abdul Ghani Rafek 2004. *Computation or rock quality designation (RQD) using spectral analysis surface wave method.* Buletin Geological Society of Malaysia 49: 51-55.
16. Tokimatsu, K., Kuwayama, S., Tamura, S. & Miyadera, Y. 1991. Vs determination from steady state rayleigh wave method. *Soils and Foundation* 31(2):153-163.

Journal of Ocean, Mechanical and Aerospace
-Science and Engineering-, Vol.26

December 30, 2015

Determination of the Lift and Drag of 2D Planing Flat Plate Riding on the Free Surface

Amin Rezaei, Hassan Ghassemi, Esmail Noshadi,

Department of Maritime Engineering, Amirkabir University Of Technology, Tehran, Iran

* Corresponding author email: gasemi@aut.ac.ir

Paper History

Received: 12-December-2015
Received in revised form: 28-December-2015
Accepted: 30-December-2015

ABSTRACT

The behavior of planing hull is very similar to planing flat plate. So to treat the planing hull performance at moderate Froude number, 2D planing flat plate was analyzed in different Froude number between 0.5 and 1. Finite volume, using ANSYS-CFX v14 software with RNG turbulence model was used to simulate planing plate. The numerical results of the pressure distribution, free surface profile, lift and drag at different AOAs are presented and discussed. Present calculations are compared with Kramer et al [7] results and show almost good agreement.

KEY WORDS: *2D planing flat plate, RNG turbulence model, Lift, Drag, Pressure distribution.*

NOMENCLATURE

C_p	Pressure coefficient
D_t	Total drag
D_p	Pressure drag
D_w	Wave drag
D_s	Spray drag
D_f	Frictional drag
f	External force
g	Gravitational acceleration
Li	Initial immersed length
L_w	Wetted length
ε_c	Critical Strain
L_t	Total lift
L_s	Spray lift
L_p	Pressure lift
L_f	Frictional lift
u	Flow speed
U	Velocity vector
V	Pressure vector
λ	Wave length
μ	dynamic viscosity
μ_a	Air dynamic viscosity
μ_w	water dynamic viscosity
v_a	Air kinematic viscosity
v_w	Water kinematic viscosity
ρ	Density
ρ_a	Air density
ρ_w	Water density
τ	AOA (AOA)
τ_w	Wall shear stress

1.0 INTRODUCTION

Computational commercial software's play an important role in industry and economic system because investigators can reduce huge costs by using them. It is true that in marine industry experimental researches are particularly important but researchers can break costs and make more exact sample by simulation and refuse using wrong model tests. Hydrodynamic parameters and pressure distribution should be known to design a perfect planing hull. But planing hull treat like flat plate so forth investigators prefer to use planing flat plate instead of complex models to do their computational studies. 2-D planing flat plate surfaces are used for example as seaplanes, planing crafts, surface effect ship (SES) seals, thin foil without camber and water impact loads [1,2]. But in a number of these cases as SES seals, planing surface may operate at lower speeds where nonlinear effects are important and must be considered.

There are some experimental, analytical and numerical research in which the planing hull is considered as planing flat plate. Brown worked on the planing lift characteristics of rectangular flat plate and presented equations which calculate lift for all

deadrise angles [3]. Payne investigated very much on the planing flat plate and planing crafts, impact forces on those bodies, pressure distribution, etc. during 50 years from 1950-2000 [4, 5]. The influencing factors of drag reduction by air injecting to a flat-plate carried out by Ou and Dong [6].
A flow past a two dimensional flat plate at low Froude number was studied by Kramer et al (2013) [7]. The effects of viscosity and free-surface nonlinearity were concluded that nonlinear and viscous effects are important when the AOA is greater than approximately 10° and the low Froude number (means Fr<0.8). Durante et al presented a numerical model for the 2D planing surfaces using linearized potential-flow theory at finite Froude number in which the surface is replaced by a representation of the pressure distribution along the plate using triangular pressure finite elements [8]. A simple numerical approach was employed to obtained data on hydrodynamic coefficients and flow pattern for various ranges of input parameters. These data are partly verified through the analysis of two limiting cases of the considered problem: first, the infinite depth, Froude number being finite and second, finite depth with very high Froude numbers [9]. The following sections are organized as follows. Section 2 is described the problem definition. Section 3 is given the modeling and boundary conditions and also computational domain. The governing equations are described in section 4. Section 5 presents the numerical results and discussions and finally conclusions are given in Section 6.

2.0 PROBLEM DESCRIPTION

In this study, two phase flow of air and water around a flat plat considering free surface was investigated. Schematic geometry of the planing flat plate is illustrated in Fig. 1. The planing plate length and thickness are 1m and 0.04m, respectively. Initial immersed length is L_i=0.5m. So the overall wetted length will be roughly $L_B=2L_i=1m$ based on reference [7]. A fixed reference coordinate system defined 2cm upper than leading edge. The plate has an AOA (τ). It is assumed that the flat plate has a constant speed of U on the free surface and the fluid is incompressible with a density and kinematic viscosity of ρ_w and v_w, respectively. The flow speed U and AOA varied, whereas the other parameters were constant and pressure distribution, wave breaking and viscose resistance calculated based on Froude number at wet length of L_B. Different angles and speeds are presented in Table 1.

Table 1. The different angles and speeds used in this paper.

	Froude number	0.5	0.7	1.1
AOA (deg)	Speed(m/s)			
7.5	-	1.6	2.2	3.45
10	-	-	-	3.45
12	-	-	-	3.45
15	-	-	-	3.45

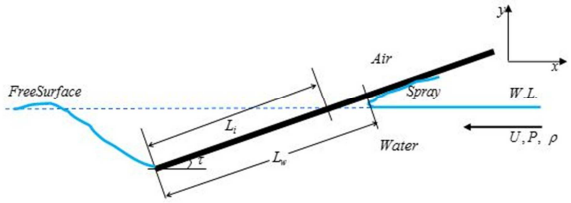

Figure.1: Problem definition.

3.0 MODELING AND BOUNDARY CONDITIONS

With attention to flat plat, computational domain should be 4L at upstream and 12L at downstream, where the L is plate length. The upper side (air) is 4L and lower side (water) is 4L, as shown in Fig. 2. This domain was meshed by 145000 quad elements as shown in Fig. 3.

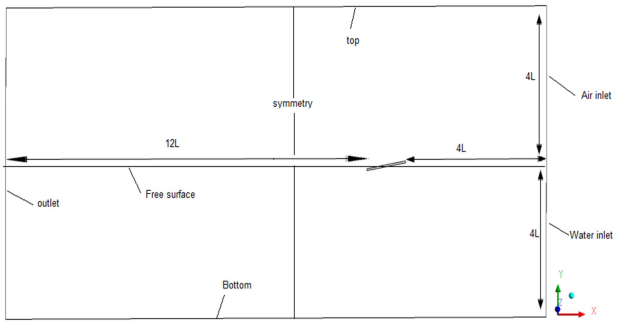

Figure.2: Domain dimensions and boundary conditions.

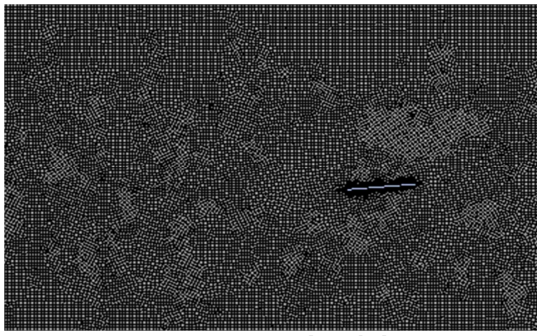
Figure.3: Computational mesh domain.

The size and type of elements play an important role in achievingcorrect results. To ensure that the results are not dependent to number of elements,the problem wassolvedfor different numbers of element at AOA of 10°. As shown in Fig. 4, the lift and drag coefficients will be constant after 125000 elements and also pressure will converge based on Fig. 5 with this number of element. These two figure show that results are mesh independent.

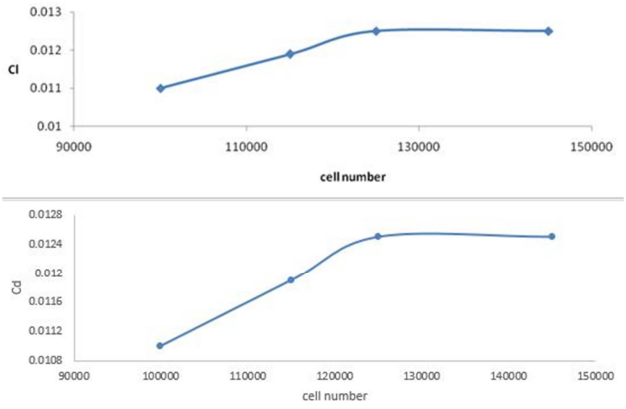

Figure.4: Effect of cell number on lift coefficient (AOA=10° and Fr= 1.1)

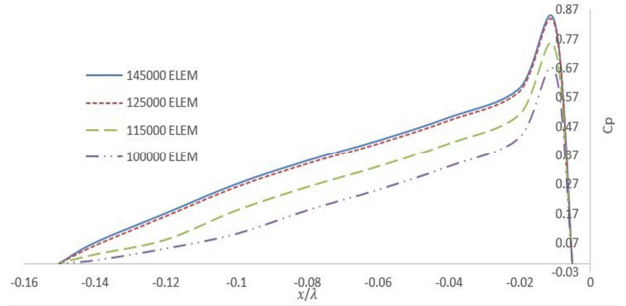

Figure.5: Convergence of presure distribution on plate for various number of element, (AOA=10 deg, Fr=1.1)

4.0 GOVERNING EQUATION

To determine fluid treatment (velocity, pressure and free surface profile) all governing equations are given as follows:

i. Continuity equation:

$$\nabla . V = 0 \quad (1)$$

ii. Navier-Stokes equations:

$$\rho\left(\frac{\partial V}{\partial t} + V.\nabla V\right) = -\nabla P + \mu\nabla^2 V + f \quad (2)$$

Where "V" and "P" are velocity vector and pressure, respectively. In addition, the factor "f" denotes external forces.

iii. Wall shear stress equation:

$$\tau = \mu\frac{\partial U}{\partial x} \quad (3)$$

where x refer to longitudinal direction. In order to obtain the volume fraction field in time, the following transport equation is solved

$$\frac{\partial \alpha}{\partial t} + \nabla.(u\alpha) = 0 \quad (4)$$

ANSYS-CFX software uses the volume fraction method to simulate the free surface. Volume fraction of a cell is its fraction of water. In this method water and air are consider as one specific fluid in which fluid density and viscosity change with parameter "a" in Eqs. (5) and (6). When a is 1 the whole cell is water and when it is 0 the whole cell is air.

$$\rho(X,t) = \alpha(X,t).\rho_w + \big(1-\alpha(X,t)\big)\rho_a \quad (5)$$
$$\mu(X,t) = \alpha(X,t).\mu_w + \big(1-\alpha(X,t)\big)\mu_a \quad (6)$$

The subscripts a and w denote air and water, respectively. In addition, x, t and μ are the spatial location vector, time variable and dynamic viscosity, respectively.

5. NUMERICAL RESULTS AND DISCUTION

In order to validation the results, pressure coefficient is compared with Kramer et al results that reported in [7] at constant AOA $\tau = 7.5°$ for various Froude numbers. Fig. 6 shows quite good agreement between simulation and Kramer's results, in which C_p and λ are:

$$C_p = \frac{P}{0.5\rho_w u^2 L_w} \quad (7)$$
$$\lambda = \frac{2\pi u^2}{g}. \quad (8)$$

where u is flow velocity in x-direction.
Hereafter, pressure distribution, free surface profile, list and drag are presented. Fig. 7 shows the pressure distribution at Fr=1.1 and AOA=10, 12 and 15 degrees. Waves generated of the free surface are shown in Figs. 8 and 9 at various AOA and Froude numbers. The height of wave and the length of wave, λ, increase by accretion in Froude number and AOA because of the relationship between flow speed and length of wave according to the equation (8).This cause in accretion of wave drag because wave energy is proportional to square of height according to equation (9) in which h is wave height.

$$E = \frac{1}{8}\rho * g * \lambda * h^2 \quad (9)$$

Also, it should be mentioned that when the AOA is increased more height of the wave generates at downstream of the flat plate. Because the flow separates from the trailing edge of the plate and causes more trough behind of the plate.
Fig. 10 illustrates contours of water velocity around plate. It is shown that velocity on the plate (near the wall) is zero because of no-slip boundary condition. Besides that, due to Fig 11 pressure is maximum in this region because of the decelerating of the velocity at leading edge of the flat plate. Lift and drag coefficients increase with Froude number and AOA. The major portion of lift and drag caused by pressure and viscose portion is neglect in comparison with pressure. This is a result of this fact that rate of

change of velocity ($\frac{\partial U}{\partial y}$) is negligible, as shown in Fig. 10.

Results of the lift and drag at various Froude number and various AOA are given in the Tables 3 and 4. The pressure drag and viscous drag components are also presented. Table 3 is given at various Froude numbers but the AOA is constant 7.5 deg. While Table 4 is shown the results at Fr=1.1 but AOA is 10, 12 and 15 degrees. The same data are presented in Figs. 12 and 13. Data of the Table 3 is demonstrated in Fig. 12 and Table 4 is related to Fig. 13.

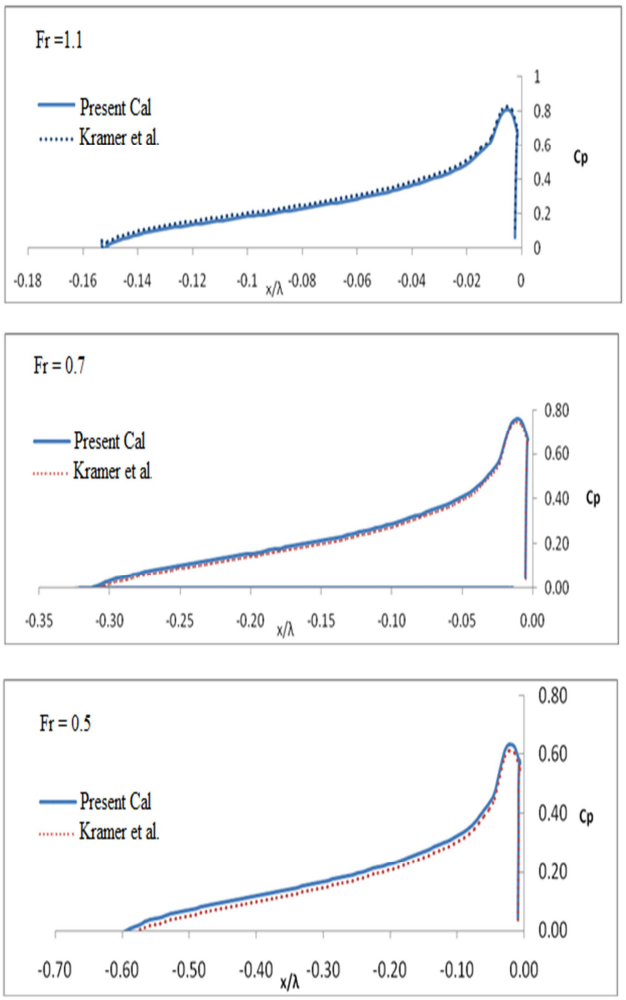

Figure.6: Comparison of pressure distribution coefficient between present calculation and Kramer et al. [7], AOA = 7.5°.

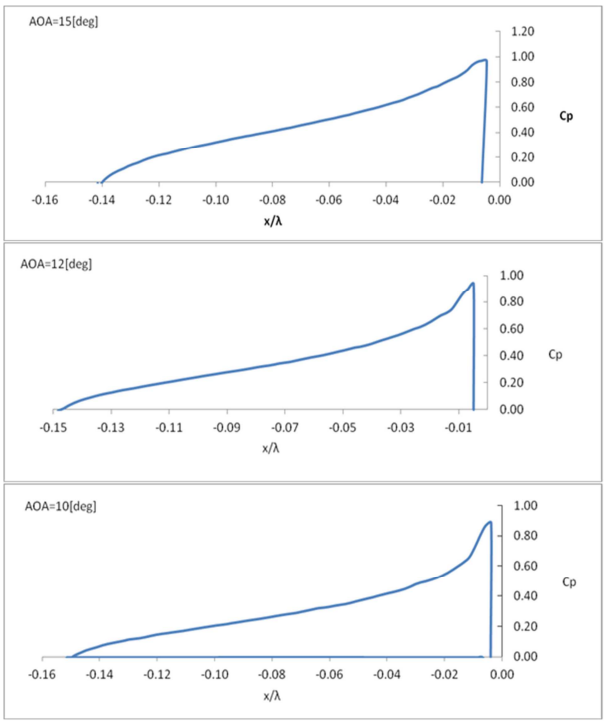

Figure.7: Pressure distribution coefficient as a function of plate length to wave length ratio for different AOA.

Table 3 Components of lift and drag in different Froude number (AOA = 7.5°)

Fr	Lift (N)	Pressure lift (N)	Drag (N)	Pressure drag (N)	Viscose drag (N)
0.5	21	21.16	9.8	9.76	0.05
0.7	28	28.07	12.1	11.39	0.04
1.1	35	36.01	15	14.97	0.03

Table.4: Components of lift and drag coefficient in different AOA (Fr=1.1.)

AOA [deg.]	Lift (N)	Pressure lift (N)	Drag (N)	Pressure Drag (N)	Viscose Drag (N)
10	63.98	64.04	16.66	16.32	0.34
12	72.02	72.07	20.24	20.04	0.2
15	97.67	97.72	30.2	29.9	0.3

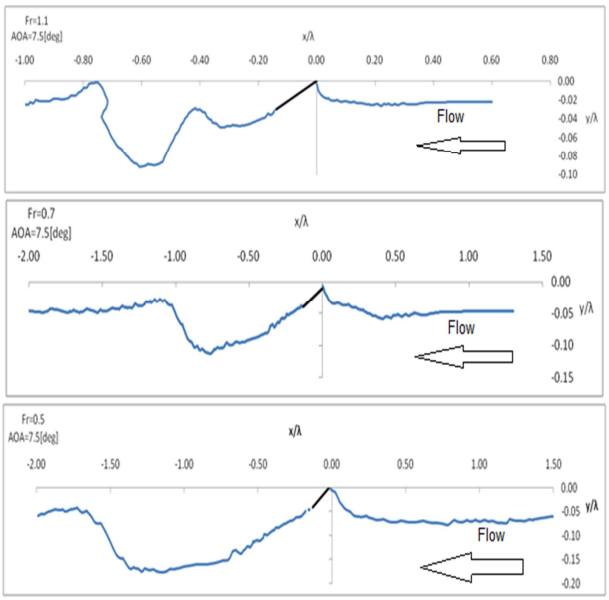

Figure.8: Plots of free-surface profile at different Fr, (AOA=7.5 deg)

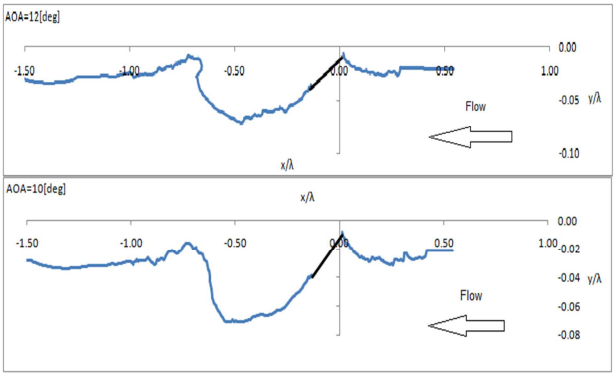

Figure.9: Plots of free-surface profile at different AOA (Fr=1.1)

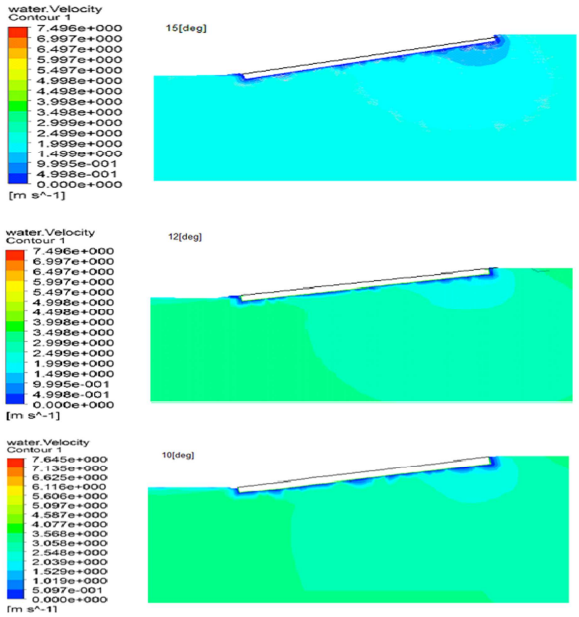

Figure.10: Velocity contours at fixed Fr= 1.1 for varying AOA

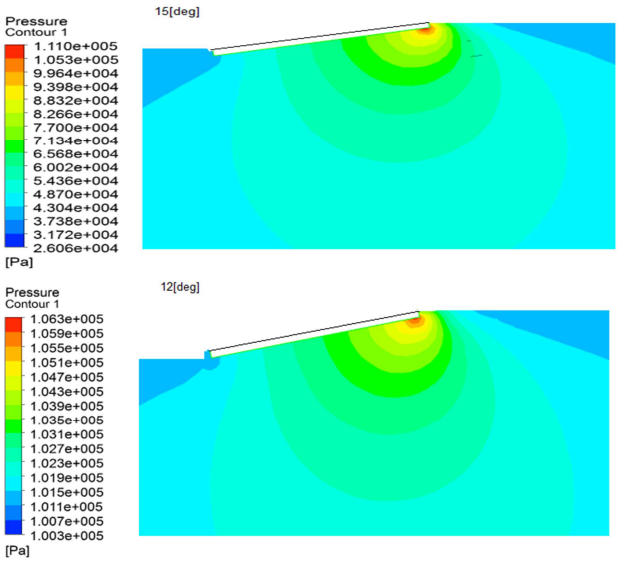

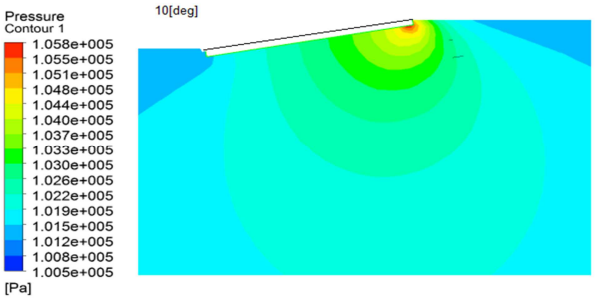

Figure.11: Plots of pressure contours for various AOA (Fr= 1.1)

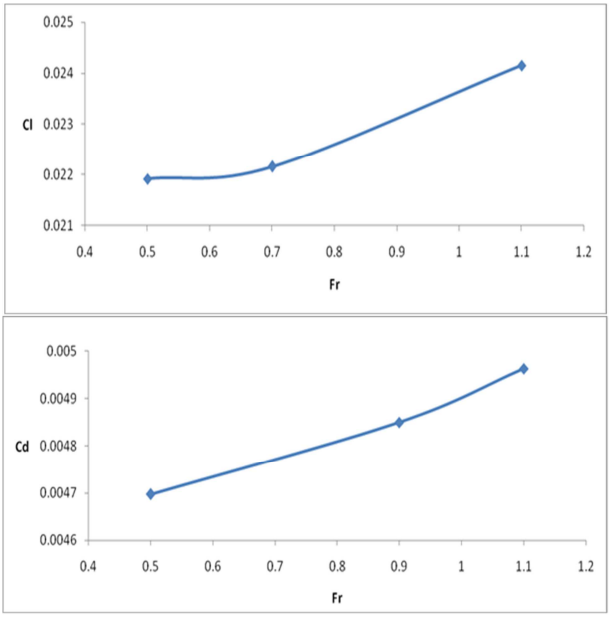

Figure.12: a) Lift coefficient as a function Fr at AOA=7.5°.
b) Drag coefficient as a functions of Fr, AOA = 7.5°.

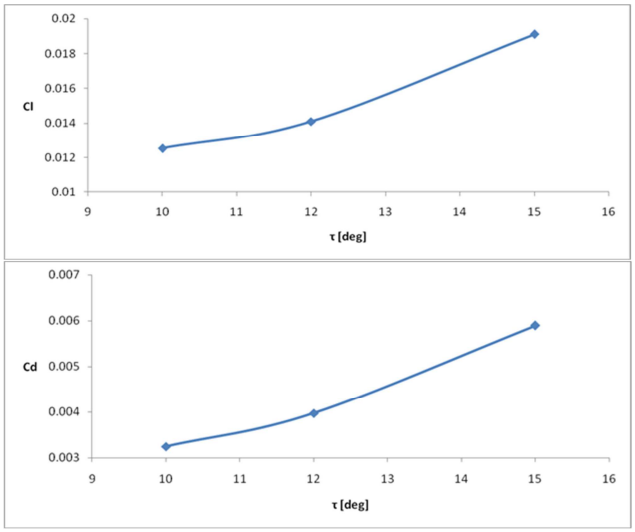

Figure.13: a) Lift coefficient as a function of AOA
b) Drag coefficient as a functions of AOA (Fr= 1.1)

6.0 CONCOLUSION

Numerical computations were conducted in this study for planing flat-plate, and pressure distributions, lift and drag, wave surface were predicted. Mesh dependency is shown that for the resent method 140000 meshes are enough. Pressure distribution is well matched with Kramer et-al results. Free surface profiles are determined at various Froude number and AOAs. High pressure is predicted at leading edge of the plate and low pressure at trailing edge. At high Froude number, it is clear observed that more free surface disturbances is shown at downstream of plate.

REFRENCES

[1]. Doctors, L. J. 2009. *A study of the resistance characteristics of surface-effect-ship seals. Proc high-Performance Marine-Vehicle Symposium*, Linthicum, Maryland.
[2]. Faltinsen, O. M. 2005. *Hydrodynamics of high-speed marine vehicles*, Cambridge University Press.
[3]. Brown P.W. 1954. *An Empirical Analysis of the Planing Characteristics of Rectangular Flat-Plates and Wedges*. Aeronautical Research Council.
[4]. Payne, P. R. 1982. *The differences between a wing and a planing plate in two-dimensional flow*. Ocean Engineering VOL 9, PP: 441-453.
[5]. Payne, P. R. 1990. *Planing and impacting plate forces at large AOAs*. Ocean Engineering,17, PP: 201-233.
[6]. Ou, Y. & Dong, W., 2012. Study on influencing factors of drag reduction by air layer to a flat-plate with bottom step. *The Twenty-second International Offshore and Polar Engineering Conference, International Society of Offshore and Polar Engineers.*
[7]. Kramer, M., Maki, K. & Young, Y. 2013. *Numerical prediction of the flow past a 2-D planing plate at low Froude numbe*r. Ocean Engineering, 70, PP: 110-117.
[8]. Durante, D., Broglia, R., Maki, K. J. & Di Mascio, A. 2014. *A study on the effect of the cushion pressure on a planing surface.* Ocean Engineering, 91, PP: 122-132.
[9]. Fridman, G. & Tuck, E. 2006. *Two-dimensional finite-depth planing hydrofoil under gravity*. Proc. Third International Summer Scientific School, “High Speed Hydrodynamics and Numerical Simulation”, Kemerovo, Russia.

Publishing

ISOMAse
Resty Menara Hotel
Jalan Sisingamangaraja No.89
Pekanbaru-Riau, INDONESIA
http://www.isomase.org/

Editing

Building P-23, Room: 314
Department of Aeronautics,
Automotive & Ocean Engineering,
Faculty of Mechanical, Universiti
Teknologi Malaysia, MALAYSIA
http://web1.fkm.utm.my/

ISSN: 2354-7065

Publication

Teknik Mesin
Fakultas Teknik,
Universitas Riau, INDONESIA
http://www.unri.ac.id/en

Organizing

Ocean & Aerospace Research
Institute, Indonesia
Pekanbaru-Riau, INDONESIA
http://isomase.org/OCARI.php/

Supporting

Mechanical Chapter of the
Institution of Engineers,
INDONESIA

Malaysian Joint Branch Royal
Institution of Naval Architects &
Institute of Marine Engineering,
Science and Technology
-Southern Chapter (MJB RINA
&IMarEST – SC)-